ESKİŞEHİR TEKNİK ÜNİVERSİTESİ BİLİM VE TEKNOLOJİ DERGİSİ B- TEORİK BİLİMLER

Eskişehir Technical University Journal of Science and Technology B- Theoretical Sciences

2024, 12(1), pp.22 - 31, DOI: 10.20290/estubtdb.1346741

RESEARCH ARTICLE

INTERACTIONS OF ANTIDEPRESSANT ESCITALOPRAM WITH ACETIC ACID AND LACTIC ACID: DFT AND MOLECULAR DOCKING ANALYSES

Cemal PARLAK [1,*] and İlkin YÜCEL ŞENGÜN [2]

[1] Department of Physics, Science Faculty, Ege University, Izmir, 35040, Turkey
[2] Food Engineering Department, Engineering Faculty, Ege University, Izmir 35040, Turkey

ABSTRACT

Many possible drugs have taken their places in the world market for the treatment of various medical diseases. Drug interactions involve combinations with drugs or other substances that alter the effect of a drug on the body. In this research, by using density functional theory, quantum theory of atoms in molecules, and in silico molecular docking against the receptor for antidepressant, we have investigated possible outcomes if antidepressant escitalopram comes across with an organic acid as acetic or lactic acids. The results suggest that escitalopram and acetic or lactic acids can interact spontaneously without requiring extra energy and depending on the interaction site different stabilities and reactivities are possible. Further, the findings show potential improvement in the effectiveness of antidepressant after interacting.

Keywords: Escitalopram, Drug interactions, DFT, Molecular docking

1. INTRODUCTION

A drug interaction is known as a reaction between a drug and a food, herb, beverage, supplement or between two or more drugs. These kinds of interactions can either produce desired or undesired results [1-3]. Escitalopram (ESCI), approved for medical use in 2002, is an antidepressant of the selective serotonin reuptake inhibitor. ESCI is mainly employed for the treatment of depression, general anxiety and panic disorder [4,5]. The investigations showed that ESCI may be more successful compared to many other antidepressants for the acute phase of the treatment, particularly with higher tolerance and acceptability [6]. In 2020, with more than 30 million prescriptions, it was the fifteenth most commonly prescribed drug in the US [7].

Lactic acid (LA) which is a chiral organic acid has biological significance owing to its function as a metabolite. LA, a normal intermediate in sugar fermentation, is made after the anaerobic metabolism of glucose in eukaryotic cells [8-9]. LA has been used in the production of solvents, metal pickling, and food additives, as an additive in various pharmaceutical products and as an emollient and keratolytic agent in various cosmetic products [10-12]. Acetic acid (AA) is produced and excreted by acetic acid bacteria, acetobacter or clostridium acetobutylicum found universally in foodstuffs, water and soil [13]. AA which gives vinegar its characteristic odor is produced by the acetification of alcohol and is an important chemical reagent and industrial chemical [14] as well it is also a biologically important metabolic intermediate and is found naturally in body fluids and plant juices.

All 5-hydroxytryptamine (5HT) receptor is the only pentameric ligand-gated ion channel found in the central and peripheral nervous systems whereas 5-hydroxytryptamine type-3 ($5HT_3$) differs markedly in structure and mechanism from the other 5HT receptors which are all G-protein-coupled. This family,

*Corresponding Author: cemal.parlak@ege.edu.tr
Received: 20.08.2023 Published: 27.02.2024

in mammals, contains serotonin, glycine, acetylcholine, γ-aminobutyric acid receptors and zinc-activated ion channels [15]. $5HT_3$ receptor has played an important role in the pathophysiology of neuropsychiatric disorders including anxiety, depression, schizophrenia and drug use and is linked to the improvement of health problems such as depression [16].

Density functional theory (DFT) has been widely used for the examination of molecular structure and physical, chemical, or biological properties of different types of compounds [17-19]. Furthermore, the quantum theory of atoms in molecules (QTAIM) has been extensively employed to enlighten the covalent and non-covalent atom-atom interactions [20, 21]. For drug discovery molecular docking technique has become an increasingly important tool. It can be used to model the interaction between small molecules (ligands, drugs) and proteins (receptors) at the atomic level. It characterizes the behavior of the ligand molecules in the binding site of target receptors as well as elucidates fundamental biochemical processes [22].

In 2021, the effect of ESCI on the AA-induced ulcerative colitis model was experimentally investigated in rats [23]. The results were in support of the beneficial anti-inflammatory and anti-oxidant effects of ESCI in ulcerative colitis regardless of depressive conditions. Further, in 2022, the effect of the LA bacteria capsules on small intestinal bacterial overgrowth in patients with depression and diabetes was explored [24]. The results of this study used ESCI for depression states suggested that the compound LA bacteria capsule is a boon for patients of small intestinal bacterial overgrowth with depression and diabetes and can improve immune function and ease depression symptoms and reduce fasting plasma glucose and level of inflammatory factors. Some parts of the experimental and medical studies mentioned above are related to the interaction of AA and LA molecules with the antidepressant ESCI. This study, by taking into account the interaction at the molecular level with physical and chemical parameters by using DFT and molecular docking, has aimed to create a theoretical approach in terms of drug interactions and to be a model for similar drug types. In continuation of our interest in drug interactions and molecular docking research[25, 26], the effects of the AA and LA molecules on the antidepressant ESCI have been examined by using DFT and QTAIM. Regarding the DFT calculations, the structure – activity relationship was also investigated. To gain deep insights into the interactions and to compare the interactions of ESCI with AA and LA, the compounds interacted were docked against the potential protein receptor 6HIS for antidepressants. All of the results obtained were discussed in brief.

2. CALCULATIONS

All compounds and interactions were optimized without any molecular constraints in water with the polarizable continuum model [27]. Vibrational frequency calculations were performed to see that the optimized structures converge to a certain minimum on the potential energy surface. Computations were carried out to B3LYP functional [28, 29] and 6-31G(d) basis set. B3LYP/6-31G(d) can be used to investigate the binding energy and reactivity properties for such interactions of the compounds compared to the highly demanding B3LYP-D3 functional or cc-pvdz basis set [30]. Binding energies (E_b) and reactivity parameters were calculated as in previous studies [17, 25, 31, 32]. For the E_b computations, the basis set superposition errors (BSSE) were considered by the counterpoise correction method [33]. Band gap energies (E_g) were taken as magnitudes of differences between the highest occupied and lowest unoccupied molecular orbitals (HOMO and LUMO). Gaussian and Multiwfn programs were used for the DFT and QTAIM calculations correspondingly whereas GaussView was used to construct the examined structures [34-36].

In order to analyse the protein–ligand interactions, docking computations were performed by AutoDock software [37]. X-ray crystal structure of the protein was obtained from RCSB-PDB [38] encoded with 6HIS for $5HT_3$ [39]. After removing water molecules from the protein, polar hydrogen atoms and Kollman charges were evaluated whereas for the compounds randomized starting positions, Gasteiger

charges, optimizations and torsions were performed. Lamarkian genetic algorithms were used in the docking process. Docking graphics were evaluated by the discovery studio visualizer [40].

3. RESULTS and DISCUSSIONS

Investigated configurations of the couples ESCI…AA and ESCI…LA were presented in Figure 1. OH…C≡N, OH…F, OH…N and OH…O interactions between the atoms of ESCI and AA or LA. Figure 1 also gives the optimized structures of OH…N site interactions encoded with III…I of both couples. All the interactions were examined and the important results were discussed and presented in brief.

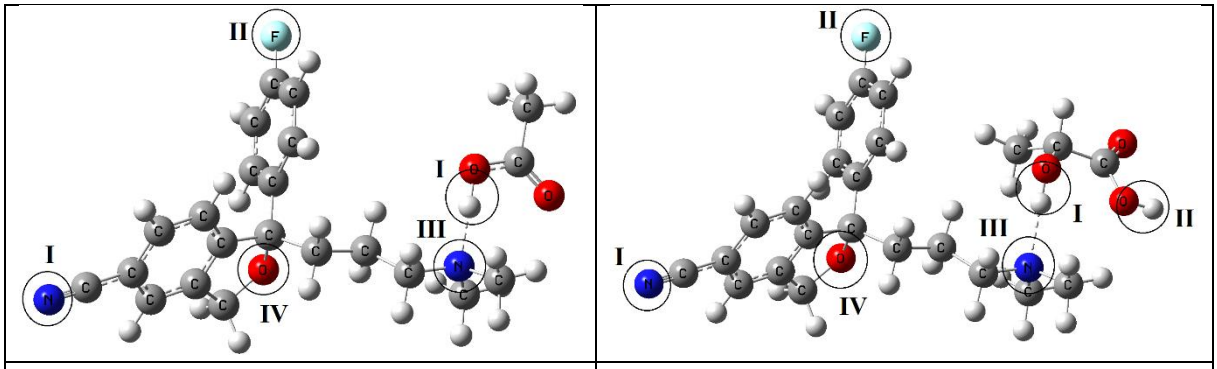

ESCI…AA | ESCI…LA

Figure 1. Encoding of interactions investigated and examples of some optimized structures.

3.1. ESCI…AA interactions

Binding energies of the interacted systems between C≡N, F, N, O atoms of ESCI and OH group of AA were found as -4.44, -1.62, -8.40 and -4.05 kcal/mol (Table 1) respectively and the OH…N (III…I) interaction is stronger than others. Following this interaction between the compounds, the OH stretching band of AA shifted from 3679 cm^{-1} to 2497 cm^{-1} and the intensity of it increased from 74.7 to 3724.2. The red-shift around 1182 cm^{-1} indicates a strong intermolecular hydrogen bond (HB) interaction. In this case, the C=O stretching vibration of AA at the interaction site shifted from 1819 cm^{-1} to 1764 cm^{-1}. The related intensity decreased from 447.6 to 441.8. The OH bond length increased from 0.977 Å to 1.038 Å whereas the C=O bond length shifted from 1.215 Å to 1.225 Å correspondingly. In the OH…N interaction region, it is obvious that the O atom of the C=O group of AA interacts with the H atom of the CH_3 group attached to the N atom of ESCI. The magnitudes of the COH angle and COH…N dihedral angle for OH…N interaction are found to be 110.35º and 179.68º respectively.

Table 1. Binding energies (kcal/mol) of the investigated interactions.

Interaction	Type	E_b	Corrected E_b
ESCI…AA			
I…I	OH…C≡N	-5.70	-4.44
II…I	OH…F	-4.94	-1.62
III…I	OH…N	-12.39	-8.40
IV…I	OH…O	-7.60	-4.05
ESCI…LA (1)			
I…II	OH…C≡N	-4.36	-2.81
II…II	OH…F	-4.12	-0.15
III…II	OH…N	-8.90	-4.75
IV…II	OH…O	-6.05	-1.83
ESCI…LA (2)			
I…I	OH…C≡N	-6.36	-5.04
II…I	OH…F	-3.99	-1.30
III…I	OH…N	-17.45	-13.07
IV…I	OH…O	-8.60	-4.17

In this configuration, QTAIM results suggest three possible HBs occurred between OH…N, H (CH_3)…O=C and H (another CH_3)…O=C and the strongest interaction takes place at the OH…N site with a value of E_{HB} = -16.56 kcal/mol. At this interaction site, the Laplacian of electron density ($\nabla^2\rho$: 0.1278 a.u.) was found as positive while the value of electronic energy density (H: -0.010 a.u.) showed a negative value showing a partially covalent interaction [25].

The reactivity parameters of the compounds and interactions as electron affinity ($-E_{LUMO}$), ionization energy ($-E_{HOMO}$), band gap (E_g), electronegativity (χ), hardness (η), chemical potential (μ) or Fermi energy and electrophilicity index (ω) are given in Table 2. The magnitudes of HOMO-LUMO energy differences were calculated as 7.817 and 4.327 eV for AA and ESCI correspondingly. For the OH…N site interaction, the E_g value of the coupled system was computed as 5.122 eV which is higher than the E_g value of ESCI and lower than the E_g value of AA. Therefore, it can be concluded that the reactivity of the interacted system is higher than single isolated AA whereas it is lower than single isolated ESCI. However, for the OH…C≡N, OH…F and OH…O interactions, E_g values reduced to 4.172, 4.320 and 4.288 eV, respectively, indicating an increase in the reactivity of ESCI…AA.

Table 2. Reactivity parameters of the compounds and interactions.

Molecule	**E_{LUMO}**	**E_{HOMO}**	**E_g**	**χ**	**η**	**μ (E_F)**	**ω**
ESCI	-5.788	-1.461	4.327	3.625	2.164	-3.625	3.036
AA	-7.609	0.208	7.817	3.701	3.909	-3.701	1.752
LA	-7.221	0.021	7.242	3.600	3.621	-3.600	1.790
Interaction	**ESCI…AA**						
OH…C≡N	-5.790	-1.618	4.172	3.704	2.086	-3.704	3.288
OH…F	-5.789	-1.469	4.320	3.629	2.160	-3.629	3.049
OH…N	-6.594	-1.472	5.122	4.033	2.561	-4.033	3.176
OH…O	-5.803	-1.515	4.288	3.659	2.144	-3.659	3.122
	ESCI…LA (1)						
OH…C≡N	-5.791	-1.641	4.150	3.716	2.075	-3.716	3.327
OH…F	-5.790	-1.478	4.312	3.634	2.156	-3.634	3.063
OH…N	-6.246	-1.493	4.753	3.870	2.377	-3.870	3.150
OH…O	-5.790	-1.524	4.266	3.657	2.133	-3.657	3.135
	ESCI…LA (2)						
OH…C≡N	-5.791	-1.591	4.200	3.691	2.100	-3.691	3.244
OH…F	-5.788	-1.475	4.313	3.632	2.157	-3.632	3.058
OH…N	-6.314	-1.467	4.847	3.891	2.424	-3.891	3.123
OH…O	-5.781	-1.503	4.278	3.642	2.139	-3.642	3.101

3.2. ESCI…LA Interactions

As encoded in Figure 1, LA has two OH groups for interaction. Binding energies of the interacted couples between C≡N, F, N, O atoms of ESCI and OH (1) group of LA were found as -2.81, -0.15, -4.75 and -1.83 kcal/mol, respectively, while E_b values between ESCI and OH (2) of LA were -5.04, -1.30, -13.07 and -4.17 kcal/mol (Table 1). According to the results, the OH…N interaction for both OH groups is stronger than other interactions. This interaction occurred with ESCI and the OH (2) group of LA is the strongest. For this interaction, the OH stretching band of LA shifted from 3677 cm^{-1} to 2473 cm^{-1} and its intensity increased from 96.3 to 2921.8. The change in the wavenumber is 1204 cm^{-1} and the change in infrared intensity is around 2825 addressing a very strong hydrogen bonding at the OH edge. Following the interaction OH bond length increased from 0.977 Å to 1.585 Å which confirms the red-shift in the IR spectrum. Furthermore, it is noteworthy that the hydrogen atom of the OH group moves to the nitrogen atom of ESCI after interaction and the NH bond length was found as 1.082 Å. In this case, the C=O stretching vibration of LA shifted from 1817 cm^{-1} to 1683 cm^{-1}. The related intensity decreased from 385.8 to 447.5. The carbonyl bond length shifted from 1.214 Å to 1.247 Å. In the OH (2)…N interaction region, it is obvious that O atom of the carbonyl group of LA interacted with the H atom of the CH_3 group attached to the N atom of ESCI. The magnitudes of the COH angle and COH…N dihedral angle for OH (2)…N interaction are found to be 108.75° and -8.15° respectively.

In this configuration, QTAIM results suggest that three possible HBs occurred as ESCI…LA and the strongest interaction takes place at the OH (2)…N site with a value of E_{HB} = -17.64 kcal/mol. For this interaction, $\nabla^2\rho$ (0.1772 a.u.) was found as positive while the value of H (-0.0059 a.u.) showed a negative value addressing a partially covalent interaction [20, 25].

As seen from Table 2, band gap values were calculated as 7.242 and 4.327 eV for LA and ESCI, respectively. For the OH (2)…N site interaction, the value of band gap energy for the coupled system was calculated as 4.847 eV which is higher than the E_g value of ESCI and lower than the E_g value of LA. Therefore, it can be concluded that the reactivity of the coupled system is higher than single isolated LA while it is lower than single isolated ESCI. For the other interactions, however, E_g values reduced to 4.200, 4.313 and 4.278 eV indicating an increase in the reactivity of ESCI…LA. A similar trend is observed for electronegativity, hardness and Fermi energy as well.

3.3. Molecular Docking

Molecular docking results on the couples ESCI…AA and ESCI…LA with the protein 6HIS for the $5HT_3$ receptor are herein reported together with the data for the drug ESCI [25]. Docking results for ESCI & 6HIS, ESCI…AA & 6HIS and ESCI…LA & 6HIS interactions are given ten binding poses ranked from the lowest to the highest energetic conformation and the related energy ranges are –6.19 to –5.51, –7.38 to –5.97 and –7.07 to –4.95 kcal/mol, respectively. The best conformer for each docking was chosen based on the most favourable docking score and the presence of non-covalent bonding interactions.

The results of the lowest binding and decomposed energies are given in Table 3. Approximate binding free energy (ΔG) is the sum of the terms; dispersion/repulsion (ΔG_{vdW}), hydrogen bonding (ΔG_{Hbond}), electrostatic energy (ΔG_{elec}), deviation from the covalent geometry ($\Delta G_{conform}$), restriction of internal rotors, global rotation and translation (ΔG_{tor}), desolvation and hydrophobic effect (ΔG_{desolv}). The best poses docked in receptors are given in Figure 2.

Table 3. Lowest binding energy (kcal/mol) and the decomposed component terms.

Structure	ΔG	$\Delta G_{vdW}+\Delta G_{Hbond}+\Delta G_{desolv}$	ΔG_{elec}	$\Delta G_{intermol}$	$\Delta G_{tot\ int}$	ΔG_{tor}	$\Delta G_{unbound}$
ESCI & 6HIS [25]	–6.19	–6.43	–1.25	–7.68	–1.19	+1.49	–1.19
ESCI…AA & 6HIS	–7.38	–9.71	–0.06	–9.77	–1.65	+2.39	–1.65
ESCI…LA & 6HIS	–7.07	–8.79	–1.26	–10.05	–2.66	+2.98	–2.66

The values of free lowest binding energies for docking ESCI…AA and ESCI…LA against the protein 6HIS were calculated as –7.38 and –7.07 kcal/mol correspondingly. All the compounds show very good binding for the receptor 6HIS. However, the magnitudes of free binding energies of the complexes are higher than the drug ESCI alone which is referring to a stronger interaction for the complexes.

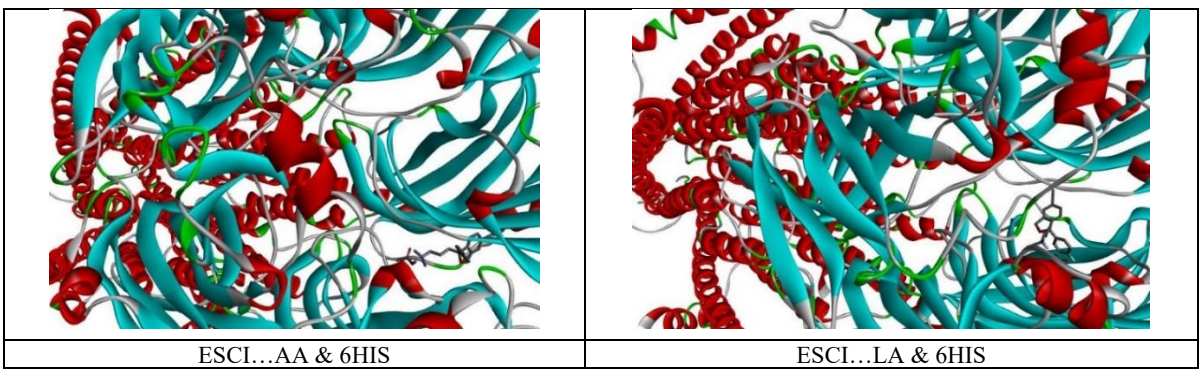

ESCI…AA & 6HIS | ESCI…LA & 6HIS

Figure 2. Best poses of the complexes docked in 6HIS.

In our previous study, the docking of the drug ESCI alone indicated three hydrogen bonding interactions with the amino acid residues of 6HIS as Asn_{A50}, Val_{A51} and Tyr_{A223} as well as some hydrophobic interactions [25]. Due to the successful results in binding energy and hydrogen bonds in the docking of ESCI with 6HIS, the same grid parameters in the receptor were considered for the complexes. Under the same docking conditions, as for ESCI…AA docked in 6HIS, the results have shown three hydrogen bonding interactions through both its drug ESCI and AA, namely one hydrogen bond of 3.89 Å linking the drug ESCI to Arg_{A65} amino acid, as well as two interactions formed between AA and Trp_{A63} or Ile_{B100} (of 5.08 and 6.20 Å correspondingly).

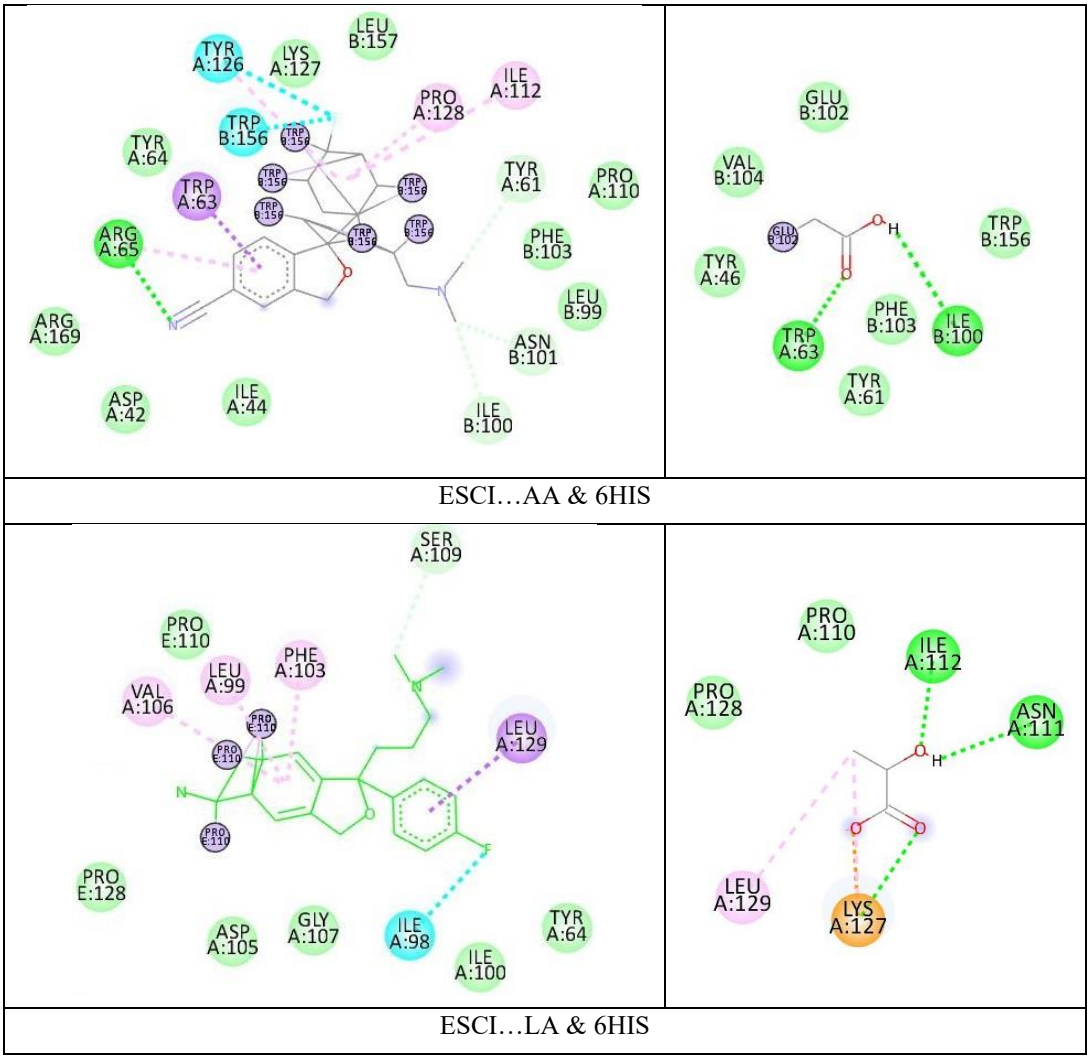

Figure 3. 2D interactions of ESCI, AA and LA with the amino acids of 6HIS.

ESCI is involved a π–π stacking with Trp_{A63}. Hydrophobic interactions as π, alkyl and mixed π/alkyl are showed around ESCI as Tpr_{A63}, Pro_{A128}, Ile_{A112}, Tyr_{A126} and Arg_{A65} residues in the ESCI…AA case as displayed in Figure 3. Furthermore, van der Waals (Asp_{A42}, Ile_{A44}, Tyr_{A64}, Lys_{A127}, Leu_{B157}, Phe_{B103}, Leu_{B99}, Pro_{A110} and Arg_{A169}), non-classical carbon hydrogen bonds (Tyr_{A61}, Asn_{B101} and Ile_{B100}), covalent bond (Trp_{B156}) and halogen interactions (Tyr_{A126} and Trp_{B156}) have been seen between the ESCI and residues of 6HIS whereas some interactions such as van der Waals (Tyr_{A46}, Val_{B104}, Glu_{B102}, Phe_{B103}, Trp_{B156} and Tyr_{A61}) and covalent bond (Glu_{B102}) interactions are found for AA and residues.

For ESCI…LA docked in 6HIS, three hydrogen bonding interactions between LA and amino acids Asn_{A111}, Ile_{A112} and Lys_{A127} (of 3.81, 4.24 and 4.39 Å, respectively) are shown whereas the results have suggested no formation of the classical hydrogen bonding between ESCI and 6HIS. ESCI is involved in a π–σ stacking with Leu_{A129}. Hydrophobic interactions as π, alkyl and mixed π/alkyl are shown around ESCI as Leu_{A99}, Phe_{A103}, Leu_{A129}, and Val_{A106} amino acids (Figure 3). Moreover, van der Waals interactions (Asp_{A105}, Gly_{A107}, Ile_{A100}, Try_{A64}, Pro_{E110} and Pro_{E128}), non-classical carbon hydrogen bond (Ser_{A109}), covalent bond (Pro_{E110}) and halogen interaction (Ile_{A98}) are showed between the ESCI and residues of 6HIS while van der Waals (Pro_{A110} and Pro_{A128}), alkyl hydrophobic (Leu_{A129} and Lys_{A127}) and electrostatic attractive charge (Lys_{A127}) interactions are found for LA and residues.

When evaluating all docking results, ESCI…AA and ESCI…LA couples show very good binding for the protein 6HIS. It indicates that the associations of AA and LA with the drug ESCI might enhance their antidepressant-like action. In addition, these results agree with existing experimental results [23, 24]. Further, the ESCI…AA interaction is found theoretically to be performing better than the drug ESCI alone and ESCI…LA couple docked in 6HIS.

4. CONCLUSION

In the present research, the most possible interaction sites and mechanisms of ESCI with AA and LA and some important structural parameters, and diagnostic vibrational bands and chemical reactivities of interacted couples were investigated by DFT and QTAIM. Further, the protein – ligand binding interactions between 6HIS and the interacted couples were simulated by the molecular docking method. The results suggest that OH…N site interaction for both ESCI…AA and ESCI…LA is the most stronger based on the binding energy calculations whereas OH…N≡C sites are found to be more reactive than others. The most reactive and the most stable interactions would be preferable for the purpose of use. Molecular docking results indicate that both associations might enhance the ESCI antidepressant-like action. Further, ESCI…AA & 6HIS association has performed better than the drug ESCI alone and ESCI…LA docked in the binding pocket of 6HIS. In addition, it seems that the theoretical procedures carried out at the molecular level with physical and chemical parameters can complement clinical trials or medical experiments, or even venture with some confidence into experimentally unexplored territory.

CONFLICT OF INTEREST

The authors stated that there are no conflicts of interest regarding the publication of this article.

AUTHORSHIP CONTRIBUTIONS

All authors contributed equally.

REFERENCES

[1] Lanser DAC, Van der Kleij MBA, Veerman GDM, Steeghs N, Huitema ADR, Mathijssen RHJ, Oomen-de Hoop E. Design and statistics of pharmacokinetic drug-drug, herb-drug, and food-drug interaction studies in oncology patients. Biomed Pharmacother 2023; 163: 114823.

[2] Flynn E, Drug-Drug Interactions. 2007. xPharm: The Comprehensive Pharmacology Reference, Editor: Enna SJ, Bylund DB. Boston: Elsevier. 1–3.

[3] Veerman GDM, Hussaarts K, Jansman FGA, Koolen SWL, van Leeuwen RWF, Mathijssen RHJ. Clinical implications of food-drug interactions with small-molecule kinase inhibitors. Lancet Oncol 2020; 21(5): 265─279.

[4] Owens MJ, Knight DL, Nemeroff CB. Second-generation SSRIs: human monoamine transporter binding profile of escitalopram and R-fluoxetine. Biol Psychiatry 2001; 50: 345–350.

[5] Jonathan RT, Davidson MD, Bose A, Korotzer A, Zheng H. Escitalopram in the treatment of generalized anxiety disorder: double-blind, placebo controlled, flexible-dose study. Depress and Anxiety 2004; 19: 234─240.

[6] Cipriani A, Furukawa TA, Salanti G, Chaimani A, Atkinson LZ, Ogawa Y, Leucht S, Ruhe HG, Turner EH, Higgins JPT, Egger M, Takeshima N, Hayasaka Y, Imai H, Shinohara K, Tajika A, Ioannidis JPA, Geddes JR. Comparative efficacy and acceptability of 21 antidepressant drugs for the acute treatment of adults with major depressive disorder: a systematic review and network meta-analysis. Lancet 2018; 391: 1357–1366.

[7] The Top 300 of 2020. ClinCalc. Retrieved 7 October 2022.

[8] Narladkar A, Balnois E, Grohens Y. An AFM study of poly(L-lactic acid) and poly(D-lactic acid) macromolecules and their stereocomplexes at the solid-air interface. Macromol Symp 2006; 241: 34–44.

[9] Kleerebezem M, Hugenholtz J. Metabolic pathway engineering in lactic acid bacteria. Curr Opin Biotechnol 2003; 14: 232–237.

[10] Maki-Arvela P, Simakova IL, Salmi T, Murzin DY. Production of lactic acid/lactates from biomass and their catalytic transformations to commodities. Chem Rev 2014; 114: 1909–1971.

[11] Sengun Yucel I, Kilic G, Charoenyingcharoen P, Yukphan P, Yamada Y. Investigation of the microbiota associated with traditionally produced fruit vinegars with focus on acetic acid bacteria and lactic acid bacteria. Food Biosci 2022; 47: 101636.

[12] Chan BS, Endo S, Kanai N, Schuster VL. Identification of lactate as a driving force for prostanoid transport by prostaglandin transporter PGT. Am J Physiol Renal Physiol 2002; 282(6): F1097-1102.

[13] Buckingham, J. Dictionary of Organic Compounds. 1996; 1 (6th ed.). London: Chapman & Hall.

[14] Cheung H, Tanke RS, Torrence GP. Acetic Acid. Ullmann's Encyclopedia of Industrial Chemistry. 2011; Weinheim: Wiley-VCH.

[15] Nemecz A, Prevost MS, Menny A, Corringer PJ. Emerging molecular mechanisms of signal transduction in pentameric ligand gated ion channels. Neuron 2016; 90(3): 452–470.

[16] Fakhfouri G, Rahimian R, Dyhrfjeld-Johnsen J, Zirak MR, Beaulieu JM. 5-HT_3 receptor antagonists in neurologic and neuropsychiatric disorders: The iceberg still lies beneath the surface. Pharmacol Rev 2019; 71(3): 383–412.

[17] Parlak C, Alver Ö, Bağlayan Ö. Quantum mechanical simulation of Molnupiravir drug interaction with Si-doped C_{60} fullerene. Comput Theor Chem 2021; 1202; 113336.

[18] Beaula TJ, Muthuraja P, Dhandapani M, Joe IH, Rastogi VK, Jothy VB. Biological applications and spectroscopic investigations of 4-nitrophenol-urea dimer: A DFT approach. Chem Phys Lett 2016; 645: 59-70.

[19] Tamer Ö, Mahmoody H, Feyzioğlu KF, et al. Synthesis of the first mixed ligand Mn (II) and Cd (II) complexes of 4-methoxy-pyridine-2-carboxylic acid, molecular docking studies and investigation of their anti-tumor effects in vitro. Appl Organometal Chem 2020; 34: e5416.

[20] Bader RFW. In Atoms in Molecules: A Quantum Theory (Oxford: Clarendon Press), 1990.

[21] Grabowski SJ. What Is the Covalency of Hydrogen Bonding? Chem Rev 2011; 111: 2597─2625.

[22] Ferreira LG, Dos Santos RN, Oliva G, Andricopulo AD. Molecular docking and structure-based drug design strategies. Molecules 2015; 20(7): 13384-13421.

[23] Firouzabadi N, Alimoradi N, Najafizadeh M, Najafizadeh P. Effect of escitalopram on an acetic acid-induced ulcerative colitis model. Clin Exp Pharmacol Physiol 2021; 48(5): 782-790.

[24] Wei F, Zhou L, Wang Q, Zheng G, Su S. Effect of Compound Lactic Acid Bacteria Capsules on the Small Intestinal Bacterial Overgrowth in Patients with Depression and Diabetes: A Blinded Randomized Controlled Clinical Trial. Disease Markers 2022; 6721695.

[25] Daboe M, Parlak C, Direm A, Alver Ö, Ramasami P. Interaction between escitalopram and ibuprofen or paracetamol: DFT and molecular docking on the drug-drug interactions. J Biomol Struct Dyn 2024; 42(2): 672-686.

[26] Guerraoui A, Goudjil M, Direm A, Guerraoui A, Yücel Sengün I, Parlak C, Djedouani A, Chelazzi L, Monti F, Lunedei E, Boumaza B. A rhodanine derivative as a potential antibacterial and anticancer agent: Crystal structure, spectral characterization, DFT calculations, Hirshfeld surface analysis, in silico molecular docking and ADMET studies. J Mol Struct 2023; 1280: 135025.

[27] Tomasi J, Mennucci B, Cammi R. Quantum mechanical continuum solvation models. Chem-Rev 2005; 105: 2999–3094.

[28] Becke AD. Density-functional thermochemistry. III. The role of exact exchange. J Chem Phys 1993; 98: 5648-5652.

[29] Lee C, Yang W, Parr RG. Development of the Colle-Salvetti correlation-energy formula into a functional of the electron density. Phys Rev B 1988; 37: 785-789.

[30] Parlak C, Alver Ö, Bağlayan Ö, Ramasami P. Theoretical insights of the drug-drug interaction between favipiravir and ibuprofen: a DFT, QTAIM and drug-likeness investigation. J Biomol Struc Dyn 2023; 41: 4313–4320.

[31] Parr RG, Szentpaly Lv, Liu S. Electrophilicity index. J Am Chem Soc 1999: 121; 1922–1924.

[32] Padmanabhan J, Parthasarathi R, Subramanian V, Chattaraj PK. Electrophilicity-Based Charge Transfer Descriptor. J Phys Chem A 2007; 111: 1358–1361.

[33] Simon S, Duran M, Dannenberg J. How does basis set superposition error change the potential surfaces for hydrogen-bonded dimers? J. Chem. Phys. 1996; 105: 11024–11031.

[34] Frisch MJ, Trucks GW, Schlegel HB et al. Gaussian 16, Revision C.01, Gaussian Inc., Wallingford, CT. 2016.

[35] Lu T, Chen F. Multiwfn: A multifunctional wavefunction analyser. Comput Chem 2012; 33: 580–592.

[36] Dennington RD, Keith TA, Millam JM. GaussView 6.0.16, Gaussian Inc., 2016.

[37] Morris GM, Huey R, Lindstrom W, Sanner MF, Belew RK, Goodsell DS, Olson AJ. Autodock4 and AutoDockTools4: automated docking with selective receptor flexiblity. J Comput Chem 2009; 16: 2785-2791.

[38] Berman HM, Westbrook J, Feng Z, Gilliland G, Bhat TN, Weissig H, Shindyalov IN, Bourne PE. The Protein Data Bank. Nucleic Acids Research 2000; 28: 235-242.

[39] Polovinkin L, Hassaine G, Perot J, Neumann E, Jensen AA, Lefebvre SN, Corringer PJ, Neyton J, Chipot C, Dehez F, Schoehn G, Nury H. Conformational transitions of the serotonin 5-HT_3 receptor. Nature 2018; 563 (7730): 275–279.

[40] BIOVIA, Discovery Studio Visualizer Software, Version 21.1.0, San Diego 2021.